BMB
Reports

BMB Rep. 2024; 57(10): 453-458
www.bmbreports.org

Increased ER stress by depletion of PDIA6 impairs primary ciliogenesis and enhances sensitivity to ferroptosis in kidney cells

Joon Bum Kim[1,#], Hyejin Hyung[1,#], Ji-Eun Bae[2], Soyoung Jang[1], Na Yeon Park[1], Doo Sin Jo[3], Yong Hwan Kim[1], Dong Kyu Choi[1], Hong-Yeoul Ryu[1,2], Hyun-Shik Lee[1,2], Zae Young Ryoo[1] & Dong-Hyung Cho[1,3,4,]*

[1]School of Life Sciences, BK21 FOUR KNU Creative BioResearch Group, Kyungpook National University, Daegu 41566, [2]KNU LAMP Research Center, KNU Institute of Basic Sciences, Kyungpook National University, Daegu 41566, [3]ORGASIS Corp., Suwon 16229, [4]Organelle Institute, Kyungpook National University, Daegu 41566, Korea

Primary cilia are crucial for cellular balance, serving as sensors for external conditions. Nephronophthisis and related ciliopathies, which are hereditary and degenerative, stem from genetic mutations in cilia-related genes. However, the precise mechanisms of these conditions are still not fully understood. Our research demonstrates that downregulating PDIA6, leading to cilia removal, makes cells more sensitive to ferroptotic death caused by endoplasmic reticulum (ER) stress. The reduction of PDIA6 intensifies the ER stress response, while also impairing the regulation of primary cilia in various cell types. PDIA6 loss worsens ER stress, hastening ferroptotic death in proximal tubule epithelial cells, HK2 cells. Counteracting this ER stress can mitigate PDIA6 depletion effects, restoring both the number and length of cilia. Moreover, preventing ferroptosis corrects the disrupted primary ciliogenesis due to PDIA6 depletion in HK2 cells. Our findings emphasize the role of PDIA6 in primary ciliogenesis, and suggest its absence enhances ER stress and ferroptosis. These insights offer new therapeutic avenues for treating nephronophthisis and similar ciliopathies. [BMB Reports 2024; 57(10): 453-458]

INTRODUCTION

Cilia are complex cellular appendages that are composed of membranes, soluble compartments, axonemes, basal bodies, and ciliary tips (1). As both mechanical and chemical sensors, primary cilia are integral in interpreting the extracellular environment and orchestrating intricate signaling pathways that are essential for the development and maintenance of cellular homeostasis (2, 3). These cilia play crucial roles in modulating key signal transduction mechanisms that govern a wide range of cellular processes. These include the transmission of signals from molecules (4), and platelet-derived growth factor (PDGF) (5). Deficiencies in primary cilia structure and length can disrupt crucial signaling pathways and cellular functions, leading to a group of diseases that are known as ciliopathies (6). In the kidneys, these ciliopathies often result from genetic mutations that impair the ability of the primary cilia to sense fluid flow and signal effectively (6, 7). Such dysfunctions are linked to renal disorders, including polycystic kidney disease and nephronophthisis that are characterized by cyst development and advancing renal failure (8, 9).

Ferroptosis describes a distinct form of cell death, separate from traditional apoptosis and necrosis (10). Ferroptotic cell death process is intricately linked to intracellular oxidative stress, highlighting the critical need for a balanced interplay between oxidative damage and antioxidant defenses (10, 11). Accumulation of iron in cells contributes to the production of reactive oxygen species (ROS) through the Fenton reaction. The ROS attacks polyunsaturated fatty acid-rich phospholipids in cell membranes, leading to lipid peroxides accumulation and cell death (12). One of the key systems in this process is the glutathione peroxidase 4 (GPX4) pathway, which is essential for maintaining cellular redox homeostasis and preventing harmful lipid peroxide accumulation (13). This process converts lipid peroxides in cells into alcohols, which is essential for preventing ferroptosis (14, 15). Therefore, understanding the mechanisms balancing oxidative stress and antioxidant defenses is crucial for comprehending ferroptosis and its implications in pathology.

The ER is an essential organelle critical for cellular homeostasis (16). Cells react to ER stress by triggering processes like the unfolded protein response (UPR) and ER-associated degradation (ERAD) pathways. These pathways aim to correct protein folding issues or remove damaged proteins, restoring ER

*Corresponding author. Tel: +82-53-950-5382; Fax: +82-53-955-5522; E-mail: dhcho@knu.ac.kr
#These authors contributed equally to this work.

https://doi.org/10.5483/BMBRep.2023-0247

Received 26 December 2023, Revised 16 January 2024, Accepted 18 March 2024, Published online 14 May 2024

Keywords: ER stress, Ferroptosis, HK-2 cells, PDIA6, Primary cilia

ISSN: 1976-670X (electronic edition)

equilibrium (16, 17). ER stress can be induced by external stimuli, activating processes such as UPR and ERAD to counteract disruptions. ER stress management involves upstream signaling proteins that are pivotal to maintaining ER stability, but when excessively activated, can also trigger apoptosis (18, 19). A key inducer of ER stress is ROS abundance, significant in initiating ER stress responses (20, 21). Recent studies have revealed a connection between ER stress and ferroptosis. However, this relationship is complex and context-dependent, and is influenced by multiple factors (22, 23). The interplay between ER stress and ferroptosis is critical research, as it offers insights into how cellular stress responses contribute to pathological conditions.

Protein disulfide isomerase A member 6 (PDIA6), belonging to the protein disulfide isomerase (PDI) family, is essential for the formation, cleavage, and reorganization of disulfide bonds in proteins (24). Recently, PDIA6 has been identified as a potential regulator cisplatin-resistant non-small cell lung cancer (25). Nevertheless, the exact role of PDIA6 in the process of ferroptosis has yet to be elucidated. In this study, we investigated the role of PDIA6 in both primary ciliogenesis, and in ferroptosis exacerbated by ER stress.

RESULTS

To investigate the effect of PDIA6 on primary cilia, HK-2 cells were transfected with specific siRNA against PDIA6. We performed immunostaining for ARL13B, a common ciliary marker. Decreases in the number and length of primary cilia were observed in PDIA6-knockdown cells (Fig. 1A, B, Supplementary Fig. 1). Ferritin heavy chain 1 (FTH1) is a component of ferritin, which is the main iron storage protein. FTH1 is elevated in the mechanism of anti-ferroptotic effects, thereby contributing to iron metabolism. GPX4 is a major enzyme that eliminates lipid peroxidation within cells. The collapse of the GPX4 antioxidant system leads to the buildup of lipid peroxidation, which then causes ferroptotic cell death. Transferrin receptor (TFR) recognizes transferrin in the transferrin-mediated iron uptake pathway. The upregulation of TFR leads to overload of Fe^{2+}. Subsequently, excessive Fe^{2+} promotes lipid peroxidation, ultimately resulting in cell ferroptosis (26, 27). Depletion of PDIA6 indicates changes in proteins related to ferroptosis. As shown in Fig. 1C, in PDIA6-knockdown cells, the expression of FTH1 and GPX4 decreased, whereas TFR expression increased. PDIA6-knockdown cells exhibited elevated levels of ROS, as indicated by the upregulation of HO-1. DCFH-DA analysis showed consistent results to those obtained with HO-1 (Fig. 1D). Lipid peroxidation triggers ferroptosis execution. PDIA6-depleted cells were treated with lipophilic antioxidants, such as ferrostatin-1 (Fer-1) and liproxstatin-1 (Lip-1) (10, 28). C11-BODIPY is used as a sensor for lipid peroxidation in cell membranes; it binds to membranes, emitting green fluorescence that is indicative of its oxidized form. We observed an increase in the production of oxidized C11-BODIPY in PDIA6-depleted cells. However, Fer-1 significantly blocked the production of oxidized C11-BODIPY production induced by PDIA6-knockdown (Fig. 1E). 4-Hydroxynonenal (4-HNE) is a product generated during the peroxidation cascade, with increased levels in PDIA6 depletion, which were alleviated by Fer-1 treatment (Fig. 1F). Additionally, Fe^{2+} levels, indicated by FerroOrange, increased in PDIA6-knockdown cells (Fig. 1G). These results suggest that silencing PDIA6 sensitizes cells to ferroptosis. To investigate the specificity for

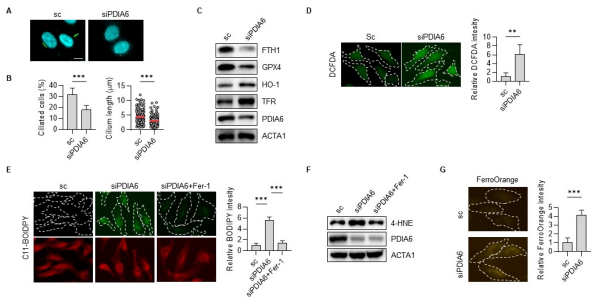

Fig. 1. Depletion of PDIA6 impairs primary cilia and sensitizes cells to ferroptosis in HK-2 cells. (A) Primary cilia were immunostained, and imaging was conducted by fluorescence microscopy. (B) The number of ciliated cells and cilia lengths are graphically represented. (C) Western blot analysis using antibodies targeting ferroptosis-related protein. (D) The fluorescence of DCFH-DA staining represents ROS. The relative intensity of DCF is graphically represented. (E) The green fluorescence of C11-BODIPY represents lipid peroxidation. The relative intensity of DCF is graphically represented. (F) Western blot analysis confirmed lipid peroxidation. (G) Intracellular Fe^{2+} levels were detected using FerroOrange, with the relative intensity of FerroOrange also being displayed graphically. Data are expressed as the mean ± SD. Statistical significance was determined using the Mann-Whitney and one-way ANOVA test, $^{**}P < 0.01$, $^{***}P < 0.001$. Scale bar: 10 μm.

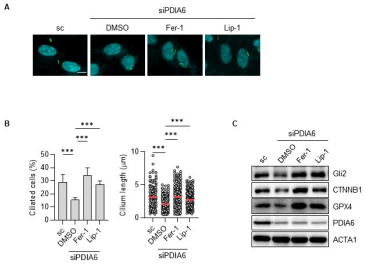

Fig. 2. Reversal of primary ciliogenesis dysregulation in PDIA6-depleted HK-2 cells by ferroptosis inhibition. (A-C) Following transfection with siRNA, cells were treated with ferroptosis inhibitors. ferrostatin-1 (Fer-1, 1 μM) and liproxstatin-1 (Lip-1, 1 μM) for 24 h. (A) Primary cilia were immunostained, and imaging was conducted by fluorescence microscopy. (B) The numbers of ciliated cells and cilia lengths are represented graphically. Measurements were taken from approximately 200 cells per group. (C) Western blot analysis using specific antibodies. Data are presented as the mean ± SD. Statistical significance was assessed using one-way ANOVA test, $^{***}P < 0.001$. Scale bar: 10 μm.

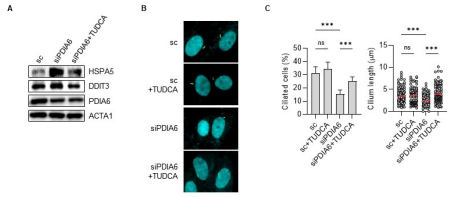

Fig. 3. Modulation of primary cilia dysregulation by inhibiting ER Stress in PDIA6-depleted cells. (A-C) Following transfection with siRNA, cells were treated with or without tauroursodeoxycholic acid (TUDCA, 10 μM) for 24 h. (A) Western blot analysis using specific antibodies. (B) Primary cilia were immunostained, and imaging was conducted by fluorescence microscopy. (C) The numbers of ciliated cells and cilia lengths are displayed graphically. Measurements were obtained from approximately 200 cells per group. Data are presented as the mean ± SD. Statistical significance was assessed using one-way ANOVA test, ns: not significant, ***P < 0.001. Scale bar: 10 μm.

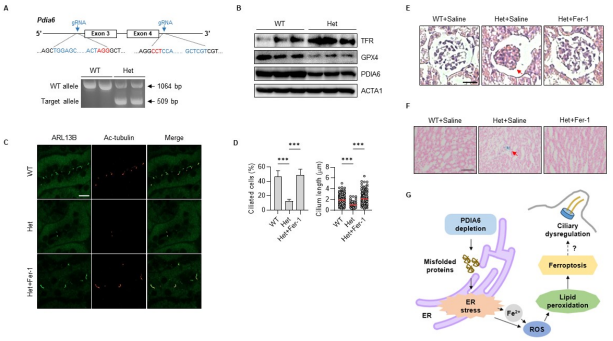

Fig. 4. Abnormal kidney morphology in PDIA6-knockdown mice. (A) The sgRNA sequences targeting *Pdia6* are highlighted in blue, and PAM sequences in red. The *Pdia6*$^{+/-}$ mice are characterized by a deletion of 58 bp in the exon 4 region. This panel shows a representative PCR genotyping for WT and *Pdia6*$^{+/-}$ mice. (B) *Pdia6* depletion enhances ferroptosis in the kidneys of *Pdia6*$^{+/-}$ mice, assessed by western blotting using specific antibodies. (C) Kidney tissues from WT and *Pdia6*$^{+/-}$ mice were immunostained with ARL13B antibody (green) and acetylated tubulin (red), and visualized using confocal microscopy. Scale bar: 10 μm. (D) The quantification of ciliated cells and cilium length are presented graphically. Measurements were obtained from approximately 200 cells per group. (E) H&E staining reveals morphological abnormalities in the glomeruli of *Pdia6*$^{+/-}$ mice, with arrows highlighting the glomeruli. Scale bar: 10 μm. (F) Perls Prussian blue staining shows iron deposition in kidney sections, particularly in the areas of the inner stripe of the outer membrane, as indicated by arrows. Scale bar: 100 μm. (G) Schematic of the PDIA6-knockdown lead to ferroptosis. Data are expressed as the mean ± SD. Statistical significance was assessed using one-way ANOVA test, ***P < 0.001.

ferroptosis, we used other forms of cell death inhibitors (Supplementary Fig. 2). To investigate whether the reduced primary cilia in PDIA6-depleted cells are associated with ferroptosis, we employed another ferroptosis inhibitor, liproxstatin-1 (Lip-1). Following treatment of ferroptosis inhibitors, we observed restored ciliary length and number in the PDIA6-knockdown group, along with the recovery of ciliary signaling proteins like Gli2 and CTNNB1 (Fig. 2, Supplementary Fig. 3). These results suggest that the dysregulation of primary ciliogenesis is linked to ferroptosis in PDIA6-depleted cells.

Recent evidence suggests that ER stress can trigger ferroptosis (23, 29), and PDIA6 depletion is known to induce ER stress (24, 30). Treatment of PDIA6-reduced cells with TUDCA, an ER stress alleviator, results in decreased HSPA5 and DDIT3 (Fig. 3A), along with restoration of the number and length of primary cilia (Fig. 3B, C, Supplementary Fig. 4). This elucidates the link between ER stress and PDIA6-mediated reduction in ciliogenesis.

We generated *Pdia6* knockout mice using CRISPR/Cas9 to target exons 3-4 of the murine *Pdia6* gene, resulting in a 58 bp deletion in exon 3, and a frameshift mutation in exon 4 of *Pdia6* $^{+/-}$ (Het) mice, as confirmed by PCR genotyping (Fig. 4A). The intercrossing of *Pdia6* heterozygous mice resulted in no homozygous offspring, suggesting the homozygous depletion of *Pdia6* is embryonic lethal on the C56BL/6J background. *Pdia6*$^{+/-}$ mice kidneys revealed increased TFR protein levels, but decreased GPX4 levels compared to WT mice (Fig. 4B). Consistently, primary ciliogenesis and ciliary elongation in proximal tubules were decreased in *Pdia6*$^{+/-}$ mice, while restoration was observed in the Fer-1-treated *Pdia6*$^{+/-}$ mice (Fig. 4C, D). In addition, the kidney pathological changes in *Pdia6*$^{+/-}$ mice were evaluated to resemble glomerulosclerosis. Following Fer-1 treatment, renal injury decreased, compared to with saline-injected *Pdia6*$^{+/-}$ mice (Fig. 4E). Perls Prussian blue staining revealed a slight increase in iron accumulation in *Pdia6*$^{+/-}$ mice compared to WT mice, while the Fer-1 injection group did not show observable iron accumulation (Fig. 4F).

Taken together, these findings suggest that PDIA6 plays a role in renal ciliogenesis and the regulation of ferroptosis, indicating that Fer-1 could significantly alleviate renal damage. We summarize the progression resulting from PDIA6-knockdown in a schematic (Fig. 4G).

DISCUSSION

Primary cilia are key to detecting extracellular signals and transducing these into cellular responses, regulating cell proliferation, migration, and differentiation. The role of primary cilia as signaling hubs for growth factors and morphogens is increasingly recognized. Consequently, mutations in cilia-associated genes lead to ciliopathies (31, 32).

In this study, we have shown that the depletion of PDIA6 disrupts primary cilia regulation via ER stress. PDIA6, which can be induced under ischemic and hypoxic conditions, plays a pivotal role in protein folding by catalyzing the formation of disulfide bonds between cysteine residues. Its levels increase in response to elevated ER stress (31). Our findings suggest that ferroptosis may be triggered by ER stress following PDIA6-knockdown, with ER stress leading to iron accumulation and lipid peroxidation. These phenomena are hypothesized to stem

from increased ROS levels driven by ER stress, which changes in transcription factors such as XBP1. Piezo1, a novel Ca^{2+}-permeable channel, has been shown to play an important role in Ca^{2+}-dependent ferroptosis. Ferroptosis can also occur through the regulation of Ca^{2+} via ER stress (33). We postulate that defects in ciliary structure arise as a consequence of ferroptosis induced under these stressful conditions. Conversely, it is also conceivable that ciliary defects might precipitate ferroptosis. Recent evidence suggests that ciliary signal transduction plays a role in regulating mRNA expression related to iron homeostasis (32). Therefore, it is possible that PDIA6-knockdown results in ciliary abnormalities and subsequent iron accumulation, culminating in ferroptosis. However, further comprehensive studies are necessary to elucidate the role of ferroptosis in primary ciliogenesis.

Mice with *Pdia6* mutation exhibit growth retardation, hypoinsulinemia, and hyperglycemia, due to the loss of pancreatic β-cell function (34, 35). A patient with PDIA6 loss-of-function gene displayed a phenotype similar to the mouse model, characteristic of ciliopathies (36). Our results suggest that PDIA6 may regulate the protein folding of ciliopathy-related proteins, either directly or indirectly.

Ferroptosis is characterized by lipid peroxidation catalysis due to ferrous iron or lipoxygenase action, leading to decreased GPX4 and cell death (37). The PERK pathway in ER stress can reduce GSH synthesis by impeding the expression of cystine/glutamate transporter via the p53 gene, thus promoting ferroptosis (38). Our findings indicate that PDIA6 suppression increases ER stress and ferroptosis. Following PDIA6 suppression, we observed increased ER stress and ferroptosis, along with reduced primary cilia. Treatment with ferrostatin-1 and liproxstatin-1, which reduce lipid peroxidation and ferroptosis, led to cilia restoration (Fig. 2). Furthermore, the use of TUDCA, a known ER stress alleviator, demonstrated the link between ER stress and cilia regulation (Fig. 3). However, more research is needed to fully understand how PDIA6 regulates primary cilia and their role in ferroptosis. Our study confirms that PDIA6 inhibition induces ferroptosis and reduces primary cilia.

Recent studies have implicated ferroptosis in kidney abnormalities (39). Previous research on *Pdia6*$^{+/-}$ mice identified syndromic disorders, including growth retardation and diabetes, but did not specifically address kidney abnormalities (34). Given the known association of primary cilia with kidney function, our study establishes a link between cilia, ferroptosis, and abnormal kidney development in mice. Intraventricular hemorrhage has observed defects in primary cilia alongside iron accumulation (40). *Pdia6*$^{+/-}$ mice displayed glomerular abnormalities that are suggestive of glomerulosclerosis. As glomerulosclerosis progresses, the abnormalities in cilia become more apparent (41). While the exact mechanisms linking ferroptosis and cilia are still unclear, these findings could provide insights into future renal disease treatment.

MATERIALS AND METHODS

Cell culture and cilia staining

HK-2 cells were maintained with RPMI (LM011-01) medium, which was supplemented with 10% FBS (S001-07) and 1% penicillin-streptomycin (LS202-02). To stain the primary cilia of HK-2 cells, they were fixed with 4% (w/v) paraformaldehyde (PFA) and 0.1% (v/v) Triton X-100. Primary cilia were immunostained with specific antibodies. Cilia images were captured using a fluorescence microscope. For each experimental condition, cilia counts were obtained from approximately 200 cells (n = 3). Cilia lengths were measured using the free-hand line selection tool in the Olympus CellSens imaging software (Olympus Europa, Hamburg, Germany).

Measurement of lipid peroxidation, ferrous iron and ROS

Intracellular lipid peroxidation was assessed using the BODIPY™ 581/591 C11 probe. The levels of cellular ferrous iron were measured using the FerroOrange probe. Intracellular ROS were measured using the dichloro-dihydro-fluorescein diacetate (DCFH-DA). All reagents were used according to the protocols provided by the manufacturers. Information about reagents used in this study is provided in the supplementary information. Fluorescence imaging was conducted using a fluorescence microscope (IX71; Olympus, Tokyo, Japan). Intensity was quantified using ImageJ software (NIH).

Animals

Pdia6 knockout mice were generated as the CRISPR/Cas9 system on the C57BL/6J genetic background. Mice were maintained under standard environmental conditions; a temperature of 20-22°C, humidity of 50-60%, light/dark cycles of 12 hours each, and free access to food and water. All animal experiments and handling procedures were performed in agreement with the guidelines of the Institutional Animal Care and Use Committee of the Kyungpook National University (Daegu, Republic of Korea). The approval license number is KNU2023-0450. The mice were divided randomly into three groups: wild-type (WT) group, heterozygous (Het) group, and Het + Ferrostatin-1 (Fer-1) group. Mice were injected intraperitoneally (i.p.) with 5 mg/kg Fer-1 in 0.9% saline once daily for consequently five days. Twenty-four hours post-injection, the animals were sacrificed for subsequent analysis.

Histological analysis

Animals were anesthetized with avertin (200 mg/kg) and transcardially perfused with PBS (pH 7.4). For immunofluorescence staining, the sectioned kidneys were incubated with the following specific antibodies at 4°C overnight, followed by incubation with secondary antibodies at room temperature for 2 hours. All images were captured on a confocal microscope. For assessment of injury, kidney tissues were stained with hematoxylin and eosin (H&E) and Perls Prussian blue to detect tissue iron. The sections were immersed in an acid solution of

potassium ferrocyanide, which reacts with ferric iron, and then counterstained with nuclear fast red. Images were acquired using a Leica microscope (Leica DMI3000B, Leica Microsystems Ltd.).

Western blotting

Cell lysates were prepared using 2×Laemmli sample buffer. The total protein content was quantified with the Bradford dye method, following the manufacturer's instructions. Kidney tissue lysates were extracted using PRO-PREP Protein Extraction supplemented with protease inhibitors. The samples were separated by SDS polyacrylamide gel electrophoresis and transferred onto PVDF membranes. The membranes were then incubated with specific primary antibodies, as detailed in the Supplementary Information.

Statistical analysis

Data were collected from a minimum of three independent experiments and are presented as means ± SD. Statistical analyses were conducted using Student's t-test and one-way ANOVA, followed by the Bonferroni post hoc test for multiple comparisons. GraphPad Prism 10 software (GraphPad Software, San Diego, CA, USA) was used for all statistical analysis, and $P < 0.05$ was considered statistically significant for all tests.

ACKNOWLEDGEMENTS

This research was supported by the National Research Foundation of Korea, funded by the Ministry of Science & ICT (2020 R1A2C2003523), and by Korea Institute for Advancement of Technology funded by the Ministry of Trade, Industry and Energy (P0025489). This research was supported by LAMP Program of the NRF grant funded by the Ministry of Education (RS-2023-00301914).

CONFLICTS OF INTEREST

The authors have no conflicting interests.

REFERENCES

1. Malicki JJ and Johnson CA (2017) The cilium: cellular antenna and central processing unit. Trends Cell Biol 27, 126-140
2. Wheway G, Nazlamova L and Hancock JT (2018) Signaling through the primary cilium. Front Cell Dev Biol 6, 8
3. Anvarian Z, Mykytyn K, Mukhopadhyay S, Pedersen LB and Christensen ST (2019) Cellular signalling by primary cilia in development, organ function and disease. Nat Rev Nephrol 15, 199-219
4. Clement CA, Ajbro KD, Koefoed K et al (2013) TGF-beta signaling is associated with endocytosis at the pocket region of the primary cilium. Cell Rep 3, 1806-1814
5. Clement DL, Mally S, Stock C et al (2013) PDGFRalpha signaling in the primary cilium regulates NHE1-dependent fibroblast migration via coordinated differential activity of MEK1/2-ERK1/2-p90RSK and AKT signaling pathways. J Cell Sci 126, 953-965
6. Ocbina PJ, Eggenschwiler JT, Moskowitz I and Anderson KV (2011) Complex interactions between genes controlling trafficking in primary cilia. Nat Genet 43, 547-553
7. Xu C, Rossetti S, Jiang L et al (2007) Human ADPKD primary cyst epithelial cells with a novel, single codon deletion in the PKD1 gene exhibit defective ciliary polycystin localization and loss of flow-induced Ca2+ signaling. Am J Physiol Renal Physiol 292, F930-945
8. McConnachie DJ, Stow JL and Mallett AJ (2021) Ciliopathies and the kidney: a review. Am J Kidney Dis 77, 410-419
9. Kolb RJ and Nauli SM (2008) Ciliary dysfunction in polycystic kidney disease: an emerging model with polarizing potential. Front Biosci 13, 4451-4466
10. Dixon SJ, Lemberg KM, Lamprecht MR et al (2012) Ferroptosis: an iron-dependent form of nonapoptotic cell death. Cell 149, 1060-1072
11. Kuang F, Liu J, Tang D and Kang R (2020) Oxidative damage and antioxidant defense in ferroptosis. Front Cell Dev Biol 8, 586578
12. Zhou Y, Lin W, Rao T et al (2022) Ferroptosis and its potential role in the nervous system diseases. J Inflamm Res 15, 1555-1574
13. Seiler A, Schneider M, Forster H et al (2008) Glutathione peroxidase 4 senses and translates oxidative stress into 12/15-lipoxygenase dependent- and AIF-mediated cell death. Cell Metab 8, 237-248
14. Yang WS, SriRamaratnam R, Welsch ME et al (2014) Regulation of ferroptotic cancer cell death by GPX4. Cell 156, 317-331
15. Friedmann Angeli JP, Schneider M, Proneth B et al (2014) Inactivation of the ferroptosis regulator Gpx4 triggers acute renal failure in mice. Nat Cell Biol 16, 1180-1191
16. Chen X and Cubillos-Ruiz JR (2021) Endoplasmic reticulum stress signals in the tumour and its microenvironment. Nat Rev Cancer 21, 71-88
17. Reggiori F and Molinari M (2022) ER-phagy: mechanisms, regulation, and diseases connected to the lysosomal clearance of the endoplasmic reticulum. Physiol Rev 102, 1393-1448
18. Tabas I and Ron D (2011) Integrating the mechanisms of apoptosis induced by endoplasmic reticulum stress. Nat Cell Biol 13, 184-190
19. Morishima N, Nakanishi K and Nakano A (2011) Activating transcription factor-6 (ATF6) mediates apoptosis with reduction of myeloid cell leukemia sequence 1 (Mcl-1) protein via induction of WW domain binding protein 1. J Biol Chem 286, 35227-35235
20. Gu S, Chen C, Jiang X and Zhang Z (2016) ROS-mediated endoplasmic reticulum stress and mitochondrial dysfunction underlie apoptosis induced by resveratrol and arsenic trioxide in A549 cells. Chem Biol Interact 245, 100-109
21. Xia S, Duan W, Liu W, Zhang X and Wang Q (2021) GRP78 in lung cancer. J Transl Med 19, 118
22. Zhao C, Yu D, He Z et al (2021) Endoplasmic reticulum stress-mediated autophagy activation is involved in cadmium-induced ferroptosis of renal tubular epithelial cells. Free Radic Biol Med 175, 236-248

23. Li X, Zhu S, Li Z et al (2022) Melittin induces ferroptosis and ER stress-CHOP-mediated apoptosis in A549 cells. Free Radic Res 56, 398-410
24. Eletto D, Eletto D, Dersh D, Gidalevitz T and Argon Y (2014) Protein disulfide isomerase A6 controls the decay of IRE1alpha signaling via disulfide-dependent association. Mol Cell 53, 562-576
25. Bai Y, Liu X, Qi X et al (2019) PDIA6 modulates apoptosis and autophagy of non-small cell lung cancer cells via the MAP4K1/JNK signaling pathway. EBioMedicine 42, 311-325
26. Chen X, Comish PB, Tang D and Kang R (2021) Characteristics and biomarkers of ferroptosis. Front Cell Dev Biol 9, 637162
27. Qian Z, Zhang Q, Li P et al (2024) A disintegrin and metalloproteinase-8 protects against erastin-induced neuronal ferroptosis via activating Nrf2/HO-1/FTH1 signaling pathway. Mol Neurobiol 61, 3490-3502
28. Zilka O, Shah R, Li B et al (2017) On the mechanism of cytoprotection by ferrostatin-1 and liproxstatin-1 and the role of lipid peroxidation in ferroptotic cell death. ACS Cent Sci 3, 232-243
29. Chen Y, Mi Y, Zhang X et al (2019) Dihydroartemisinin-induced unfolded protein response feedback attenuates ferroptosis via PERK/ATF4/HSPA5 pathway in glioma cells. J Exp Clin Cancer Res 38, 402
30. Vekich JA, Belmont PJ, Thuerauf DJ and Glembotski CC (2012) Protein disulfide isomerase-associated 6 is an ATF6-inducible ER stress response protein that protects cardiac myocytes from ischemia/reperfusion-mediated cell death. J Mol Cell Cardiol 53, 259-267
31. Mill P, Christensen ST and Pedersen LB (2023) Primary cilia as dynamic and diverse signalling hubs in development and disease. Nat Rev Genet 24, 421-441
32. Nishimura Y, Kasahara K, Shiromizu T, Watanabe M and Inagaki M (2019) Primary cilia as signaling hubs in health and disease. Adv Sci (Weinh) 6, 1801138
33. Kim YJ and Hyun J (2023) Mechanosensitive ion channels in apoptosis and ferroptosis: focusing on the role of Piezo1. BMB Rep 56, 145-152
34. Choi JH, Zhong X, Zhang Z et al (2020) Essential cell-extrinsic requirement for PDIA6 in lymphoid and myeloid development. J Exp Med 217, e20190006
35. Chhabra NF, Amend AL, Bastidas-Ponce A et al (2021) A point mutation in the Pdia6 gene results in loss of pancreatic beta-cell identity causing overt diabetes. Mol Metab 54, 101334
36. Al-Fadhli FM, Afqi M, Sairafi MH et al (2021) Biallelic loss of function variant in the unfolded protein response gene PDIA6 is associated with asphyxiating thoracic dystrophy and neonatal-onset diabetes. Clin Genet 99, 694-703
37. Xie Y, Hou W, Song X et al (2016) Ferroptosis: process and function. Cell Death Differ 23, 369-379
38. Zheng X, Liu B, Liu X et al (2022) PERK regulates the sensitivity of hepatocellular carcinoma cells to high-LET carbon ions via either apoptosis or ferroptosis. J Cancer 13, 669-680
39. Shi Y, Shi X, Zhao M et al (2023) Ferroptosis is involved in focal segmental glomerulosclerosis in rats. Sci Rep 13, 22250
40. Chen Q, Shi X, Tan Q et al (2017) Simvastatin promotes hematoma absorption and reduces hydrocephalus following intraventricular hemorrhage in part by upregulating CD36. Transl Stroke Res 8, 362-373
41. Bai Y, Li P, Liu J et al (2022) Renal primary cilia lengthen in the progression of diabetic kidney disease. Front Endocrinol (Lausanne) 13, 984452